This is "Advance Publication Article". Received Date: 6 March 2020 Accepted Date: 4 October 2020
J-STAGE Advance published Date: 25 March 2021 Journal of Prosthodontic Research

Journal of Prosthodontic Research

Official Journal of Japan Prosthodontic Society

Original article

Restoration's thickness and bonding tooth substrate are determining factors in minimally invasive adhesive dentistry

Giovanni Tommaso Rocca[a,*], Borja Baldrich[b], Carlo Massimo Saratti[a], Luis Maria Delgado[c], Miguel Roig[b], Rene Daher[a], Ivo Krejci[a]

[a] *Division of Cariology and Endodontology, School of Dentistry, University of Geneva, Geneva, Switzerland*
[b] *Department of Restorative Dentistry, Universitat Internacional de Catalunya, Barcelona, Spain*
[c] *Bioengineering Institute of Technology, Universitat Internacional de Catalunya, Barcelona, Spain*

Abstract

Purpose: To explore fracture strength and failure behaviour of minimally invasive CAD-CAM composite resin overlay restorations.
Methods: Eighty bi- and tri-layer cylindrical overlay model including the restoration bonded over bovine tooth dentin (Groups D) and enamel-dentin (Groups E) were assembled (diameter 9 mm). Restorations were milled from CAD-CAM composite resin blocks (Brilliant Crios, Coltène/Whaledent AG) in different thicknesses (0.5mm, 1mm, 1.5mm, 2mm) and equally distributed in four Groups D and four Groups E (n=10). All specimens were submitted to an Hertzian load-to-failure contact test with spherical indenter. Critical loads were recorded in Newton and data were analysed using Kruskal–Wallis test for multiple and Mann-Whitney test for 2-samples comparisons ($p < 0.05$). Fragments were examined using SEM. The stress distribution for specimens with restorations of 0.5 mm and 2 mm was also investigated with FEA.
Results: For all specimens, the mean static loads in Newton increased with an increase in restoration thickness. On contrary, restorations with the same thickness displayed higher resistance values when bonded over enamel than dentin, except for the 2-mm thick restorations. A damage competition was detected between cone/median cracks originating at the loading contact area of the restorations and radial cracks beginning at their inner surface, with the former prevailing in restorations bonded on enamel and the latter being dominant for restorations bonded on dentin.
Conclusions: For bonded ultra-thin resin composite restorations (0.5 mm to 1.5 mm) enamel as bonding substrate assures higher critical loads to fracture than dentin. This influence gradually decreases as restoration thickened.

Keywords: *Occlusal wear, Restoration, CAD-CAM, Composite resins, Fracture strenght*

Received 6 March 2020, Accepted 4 October 2020, Available online 25 March 2021

1. Introduction

Minimally invasive dentistry attempts to conserve sound tissues in order to respect the biomechanical integrity of the tooth [1]. As adhesive procedures ensure good retention of the restoration without the need for an aggressive dental tissue preparation for retentive elements, the amount of tooth structure removal is often minimal and mainly determined by the extension of the pathology. Thus, in the case of small tooth cavities, restorations can be very thin with evident concerns about the minimum thickness requirements of modern restorative materials, above all in the posterior region where stresses are higher. Manufacturer's universal recommendations for the minimal thickness of an overlay posterior restoration ranges from 1.0 to 2.0 mm, for both ceramic and resin composite materials. These thickness recommendations could significantly exceed clinical needs, leading to a larger tissue removal than required. As an example, patients affected by chemical erosion and/or mechanical attrition decrease progressively their vertical dimension of occlusion (VDO). An early re-establishment of the original VDO is crucial to protect the remaining dental structure and to recover function and aesthetics [2]. In this case, the use of bonded ultra-thin overlays (less than 1 mm) - also referred as "table-top" restorations - would be ideal to avoid invasive preparation and further tissue loss. Recently, some authors have explored the limits of modern restorative materials and in particular the in vitro relationship between their thickness and their critical load [3–5] as well as their residual strength after fatigue [6–9]. Values obtained in these studies for the minimum restoration's thickness required to withstand the normal masticatory forces are different and they depend on the type of test and material tested. For CAD-CAM lithium disilicate reinforced ceramic overlays, a wide range of values between 0.5 and 1.2 mm is recommended as minimum thickness [3,7,9–12] whereas for CAD-CAM composite resin counterparts the inferior limit of resistance lies between 0.3 and 0.6 mm [4,5,13].

A clear influence of the bonding substrate over the resistance of a ceramic restoration used in minimal thickness has been extensively demonstrated for ceramic layered structures [14–18]. In particular, if the Young's modulus of elasticity of the bonding substrate (Es) is much lower than the one of brittle coating (Ec), the latter will act under load in the same way as a glass plate placed over a flexible support, causing the appearance of tensile stresses at the inner surface of the ceramic plate. These stresses can initiate inner radial cracks in the glass undersurface, which normally spread upwards perpendicularly. These flexural radial cracks are especially dangerous and considered a main source of premature failure in ceramic dental crowns [19,20]. Critical loads needed for radial cracking increase as

* Corresponding author at: University of Geneva, CUMD School of dentistry, Department of Cariology and Endodontics, 19 Rue Lombard, 1205 Geneva, Switzerland.
E-mail address: giovanni.rocca@unige.ch (G.T. Rocca).

https://doi.org/10.2186/jpr.JPR_D_20_00008

the ratio Ec /Es reduces. Thus, core materials with high Es (glass ceramic, alumina, nickel-chromium alloy or higher) used to support thin aesthetic ceramics in crowns will improve the resistance of the coating rather than flexible substrates such as dentine or composite resins [14]. In contrast, in the case of thicker ceramic coatings over a compliant substrate, the damage starts at the ceramic surface as a cone crack (highly brittle materials) or below the plastic deformation area as a median crack (more deformable materials) and extends downwards. [19,21]. These cracks need higher critical loads to initiate and, therefore, they are considered less hazardous than radial cracks. In minimally invasive adhesive dentistry the bonding substrates that can be generally found below a bonded indirect restoration are composite resin (cavity build-up), enamel and dentine [22]. The approximate values of their E are 2.6−19.18 GPa [23], 80−100 GPa and 16−20 GPa, respectively [3,24,25]. This high elastic mismatch between enamel and dentine or composite resin suggests that the preservation of enamel as a bonding substrate in minimally invasive ceramic restorations would lead to a better supported restorative material. Guess P. et al. [7] found that whenever the preparation for a ceramic occlusal veneer exposed predominantly dentine, the risk of fracture of the thin restoration was higher than for those bonded on enamel. Nevertheless, Sasse M. et al. [9] obtained dissimilar results and a more favourable effect of dentine and composite resins as substrates for thin lithium-disilicate reinforced ceramic overlays.

Adhesion to the substrate is also contemplated within the factors influencing the fracture strength of a thin ceramic restoration. Resin bonding leads to high resistance of the ceramic coating [4,26–29].

Also, the adhesive interface has an important role during crack propagation between dissimilar elastic materials. It may deflect the fracture and impede the penetration of the crack into the substrate, saving tooth tissues [30]. This is often the case when the strength of that interface is lower than the one of the substrate (weak bonding) [31].

Recently, several CAD-CAM composite resin materials have been introduced on the market to fabricate posterior definitive restorations. A lack of literature exists on the mechanical performances of these materials when used in minimal restorative thickness [4,5,32]. Therefore, the aim of this study was to investigate the fracture resistance and the behaviour after fracture of a novel CAD-CAM composite resin material tested in different thicknesses and bonded to different tooth substrates, namely enamel-dentine and dentine. A simplified bi- and tri-layer overlay model including the restoration bonded over bovine tooth tissues was used for Hertzian contact testing. The null hypotheses tested were that both (a) the thickness of the material and (b) the tissue bonding substrate – enamel or dentine – have no impact on the load-bearing capacity and the mode of fracture of occlusal veneer restorations made out of CAD-CAM composite resin.

2. Materials and Methods

Cylindrical specimens with a diameter of 9 mm were created. The superficial layer simulated the restoration while the inner one simulated the tooth tissues (Fig. 1).

2.1. CAD-CAM resin discs fabrication

For the upper restoration layer, CAD-CAM composite resin blocks (Brilliant Crios, Coltène/Whaledent AG, Alstätten, Switzerland) with the dimension of 14x14x18 mm were sectioned perpendicularly to their longitudinal axis using a low-speed saw (IsoMet 11-1180 Low Speed Saw, Buehler Ltd, Illinois, IL, USA) to produce 80 slabs with a thickness of 0.5±0.05 mm (n=20), 1±0.05 mm (n=20), 1.5±0.05 mm (n=20) and 2±0.05 mm (n=20). Squared slabs were then reduced to discs with a diameter of 9 mm with a water-cooled drilling trephine.

2.2. Tissue cylinders fabrication

For the inner tissue layer, 80 bovine central lower incisors (n=80) stored in 0.1% thymol solution at 37 ºC, without presence of carious lesions and visible fracture lines, were buccal−lingually sectioned at the centre of the crown with a water-cooled drilling trephine resulting in 80 tissue cylinders

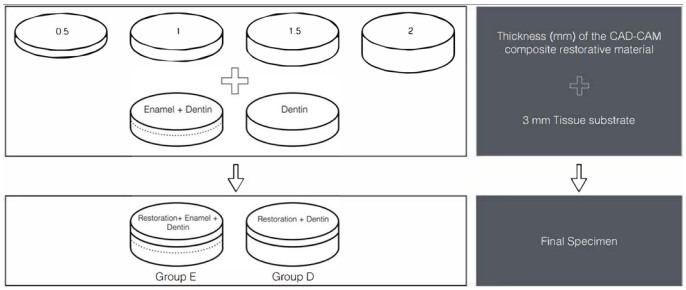

Fig. 1. Schematic representation of the specimen set-up.

(diameter 9 mm) containing, in sections, buccal enamel and dentine, the pulp chamber and palatal enamel and dentine (Fig. 2). Only enamel and dentine from the buccal part were conserved. These cylinders were first randomly distributed in two groups: enamel-dentine (E) and dentine (D). In the E group (n=40), specimens were reduced with diamond burs and then polished under cooling water using 500 grit silicon carbide paper to get a 3 mm-thick cylinder (±0.1 mm) of enamel and dentine with a flattened surface. The enamel thickness at the side of the tissue cylinder was established at 0.5±0.05 mm. In the D group (n=40), the enamel was erased with diamond burs and the superficial dentine was then flattened and polished with a 500-grit silicon paper, resulting in 3 mm-thick cylinders of dentine. When the thickness of the dentine was less than 3 mm in a section because of the former pulp chamber, a composite resin (Clearfil Majesty Posterior, Kuraray, Japan) with a similar modulus of elasticity of the dentine (Table 1) was bonded to the lower part of the dentine cylinder to fill this lack of tissues. The bonding surface with the CAD-CAM restoration was always in dentine.

The tissue cylinders of both the enamel-dentine (E) and the dentine (D) groups were randomly divided into four subgroups (n= 10) each, and associated with 0.5, 1, 1.5 and 2 mm-thick CAD-CAM resin disks (Table 2).

2.3. Luting procedures

Resin discs were submitted to an airborne-particle procedure (Kavo EWL, Type 5423, Biberach, Germany) at the inner surface with 27 µm aluminium-oxide powder at 1.5 bar pressure for 5 s at a 5 mm distance followed by an ultra-sonic cleaning bath (Biosonic UC100, Coltène/Whaledent AG, Alstätten, Switzerland) in distilled water for 5 min, following manufacturer's instructions. After drying with oil-free compressed air, a universal adhesive system was applied (One Coat 7 Universal, Coltène/Whaledent AG, Alstätten, Switzerland) over the treated surface. Discs were subsequently placed into a box (Vivapad, Ivoclar-Vivadent, Schaan, Liechtenstein) to avoid premature polymerization by ambient light. Then, for tissue cylinders of the E groups, etching of superficial enamel was performed with orthophosphoric acid 35% (Etchant Gel S, Coltène/Whaledent AG, Alstätten, Switzerland) for 30 s [33] followed by water rinsing and drying with oil-free compressed air. Subsequently, the same universal adhesive system used for CAD-CAM resin discs (One Coat 7 Universal) was applied over etched enamel (E groups) and dentine (D groups) following the manufacturer's recommendations. Adhesively treated tissue cylinders were also put under ambient light protection. A resin cement (DuoCem, Coltène/Whaledent AG, Alstätten, Switzerland) was applied between CAD-CAM resin and tissue cylinders and the latter were seated with a uniform pressure. To standardize the cement thickness during the luting procedure, two provisional composite resin wings working as support platforms were fabricated on the lateral opposite surfaces of both the resin discs and the tissue cylinders, to allow the placement of 100 µm- thick metal strips between these wings during cementation. Before curing, resin discs were seated with a 5 kg metal weight for 30 s. Excesses of cement were removed with a brush and the light-polymerization was performed with a LED lamp of 1200 mW/cm2 (Elipar S10, 3M ESPE, St Paul, MN, USA),) from the occlusal, lingual and buccal sides, 60 s per side. A water-cooled drilling

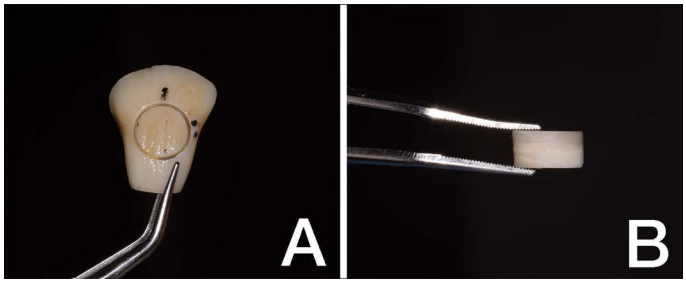

Fig. 2. Specimen preparation: A) Drilling of the tooth disc in a bovine incisor with a trephine bur. B) Final cylindrical specimen with the restoration bonded to tissues.

Table 1. Materials used in this study.

Brand name (manufacturer)	Chemical composition	Young modulus (GPa)	Poisson's ratio
Brilliant Crios (Coltène/Whaledent AG)	Cross-linked resin matrix of methacrylates reinforced by 71 wt% of barium glass (<1μm) and amorphous silica particles (<20nm)	10.3 [a]	0.24 [c]
One Coat 7 Universal Adhesive (Coltène/Whaledent AG)	10-MDP, methacrylated, polyacrylic acid, other methacrylates, photoinitiators, ethanol, water	n. a	n. a
DuoCem (Coltène/Whaledent AG)	Bis-EMA, Bis-GMA, TEGDMA, reinforced by 71%wt of barium glass silanized, amorphous silicic acid hydrophobed, inorganic filler	6.7 [a]	0.3 [b]
Clearfil Majesty Posterior (Kuraray)	Light-cure, nano-superfilled, radiopaque restorative posterior composite resin composed of nano and micro inorganic filler, silanated glass ceramic filler (average: 1.5 μm), surface treated alumina micro filler (average: 20 nm) Bis-GMA, TEGDMA, dl-camphorquinone, accelerators, pigments	22 [a]	0.22 [d]
Dentine		18.6 [c]	0.31[c]
Enamel		84.1 [c]	0.3 [c]

MDP, phosphate monomer dimethacrylate; Bis-GMA, bis-phenol A diglycidylmethacrylathe; TEGDMA, triethylenglycol dimethacrylate; Bis-EMA, ethoxylated bisphenol-A dimethacrylate; wt, weight; n.a, not available

a) From the manufacturers.
b) Li LL, Wang ZY, Bai ZC, Mao Y, Gao B, Xin HT, Zhou B, Zhang Y, Liu B. Three-dimensional finite element analysis of weakened roots restored with different cements in combination with titanium alloy posts. Chin Med J (Engl). 2006 Feb 20;119(4):305-11
c) Daher R, Feilzer AJ, Krejci I. Novel non-invasive reinforcement of MOD cavities on endodontically treated teeth. J Dent. 2016 Nov;54:77-85.
d) Papadogiannis D, Tolidis K, Lakes R, Papadogiannis Y. Viscoelastic properties of low-shrinking composite resins compared to packable composite resins. Dent Mater J. 2011;30(3):350-7. Epub 2011 May 20.

Table 2. Study design.

Groups	Substrate layer	Restoration material	Restoration thickness (mm)	Sample size
0.5E	(E) Enamel + Dentin	Brilliant Crios	0.5	n=10
1E			1	n=10
1.5E			1.5	n=10
2E			2	n=10
0.5D	(D) Dentin	Brilliant Crios	0.5	n=10
1D			1	n=10
1.5D			1.5	n=10
2D			2	n=10

trephine was finally used to remove the composite resin wings and reshape the cylinders.

2.4. Fracture strength test

Specimens were subjected to a load-to-fracture quasi-static test (Dyna-Mess, Stolberg, Germany). A stainless-steel ball-shaped indenter (diameter 5 mm) was used to apply axial compression force in the middle of the occlusal surface of the specimens. The crosshead speed was 1.0 mm/min and a compression force was applied until the specimen fractured. A 40 μm-thick foil was inserted between the contact surface of the samples (Bausch Articulating Paper, Nashua, USA) and the loading ball to reduce peak stresses at the contact point. The ultimate load-to-failure was recorded in Newtons (N) and the means and standard deviations for each subgroup were calculated.

2.5. Fractography

After fracture, all the specimens were visually examined using a stereomicroscope (SZX9, Olympus Optical Co., Tokyo, Japan). On the agreement of two examiners, types of failure were classified as: Failure type 1, when the crack broke the restoration without damaging the

subjacent tissues and provoked partial/total restoration debonding; Failure type 2, when the fracture involved both restoration and the subjacent tissues.

A selection was made in order to establish which fragments were suitable for fractographic analysis. Characteristic features such as compression curl, hackle and arrest lines were identified using the stereomicroscope. Different magnifications (ranging from 6.3x to 50x) were used depending on the size of the characteristic marks detected. Angled illumination was used to better view the fracture surface. All recognizable features were photographed and documented. Scanning electron microscopy (SEM) (Digital SEM XL20, Philips, Amsterdam, The Netherlands) was then used for more detailed analysis of the fractured surfaces. In order to remove all of the impurities, all of the fragments were cleaned in an ultrasonic 10% sodium hypochlorite bath for 3 min, rinsed with water, dried and then fixed on the support for the microscope. The specimens were gold-coated prior to the analysis with the SEM. Magnifications up to 2000x were used to obtain a higher definition of identified crack features in selected areas of interest. Accelerating voltage was set to 20.0 kV. The overall direction of crack propagation and failure origin(s) were systematically mapped for all specimens.

2.6. Finite element analysis

Four three-dimensional (3D) models were created with FEMAP (FEMAP 11.1, Siemens PLM software, Plano, Texas, USA) based on the specifications of the laboratory part of the study. Two models represented the 0.5 mm and 2 mm restorative material thickness bonded on enamel (groups 0.5E and 2E) and two models represented the 0.5 mm and 2 mm restorative material thickness bonded on dentine (groups 0.5D and 2D). The thickness of the luting cement and the enamel were set to 0.1 mm and 0.5 mm, respectively. The thickness of the dental substrate was set to 3 mm and the diameter of all the different parts was set to 9 mm as in the in vitro part of the study. A stainless-steel ball with a diameter of 5 mm was modelled, and an axial load corresponding to the mean loading force measured in the in vitro part was applied to the restorative material (Table 3). Contact regions were defined between the discs, and a bonded connector was allocated to each region except for the contact between the loading sphere and the specimens where a surface contact with a coefficient of friction of 0.25 was assigned. All materials were intended to be isotropic, homogeneous and linear elastic. The properties such as Young's modulus and Poisson's ratio were taken from the literature and assigned to each part (Table 1). The models were meshed with quadratic tetrahedral elements and three mesh refinement stages were necessary until stable stress values were reached, without excessively extending the computing time. Element size ranged between 0.1 mm and 0.5 mm and the average number of elements was 220,000 elements per model. Constraints in the x-, y- and z-directions were applied to the base of the dental substrate, and all degrees of freedom of that surface were blocked. A static analysis was performed, and the results were then compared in Nastran (NX Nastran, Siemens PLM software, Plano, Texas, USA). Maximum principal stress (MPS) values and distribution were studied from different views and sections.

2.7. Statistical analysis

Numerical data are expressed as mean ± standard deviation (SD). Analysis was performed using statistical software (Minitab version 17, Minitab, USA). One-way analysis of variance (ANOVA) was rejected because a normal distribution from each sample population was obtained (Anderson−Darling normality test) without homogeneity in the variances (Bartlett's and Levene's test). Thus, non-parametric statistics were used and consequently Kruskal–Wallis test for multiple and Mann-Whitney test for 2-sample comparisons were carried out. Statistical significance was accepted at $p < 0.05$.

3. Results

The mean loads-to-fracture in Newtons (N) registered are showed in Table 3. In relation to the different bonding substrates, both Enamel and Dentine groups showed an increase in mean load-to-failure values with an increase in restoration thickness. Conversely, restorations with the same thickness displayed higher resistance values when bonded over enamel than dentine except for the 2 mm-thick restorations. This difference decreased as the restoration became thicker (Fig 3).

Table 3. Means (SD) and coefficient of variation (CV) of the fracture strength (N) for the different groups. Groups marked with the same letter presented no significant difference.

	Restoration thickness (mm)			
	0.5	1	1.5	2
Groups E	2175,5 (246,9)^{d,e} CV: 11.35%	2561,5 (202,2)^{c} CV: 7.89%	2899,1 (474,8)^{b} CV: 16.38%	3413,2 (537,9)^{a} CV: 15.76%
Groups D	1326,2 (191,7)^{f} CV: 14.46%	2016,2 (205,9)^{e} CV: 10.21%	2412,0 (321,6)^{c,d} CV:13.33%	3325,4 (447,6)^{a,b} CV:13.46%

The majority of the specimens of Groups E displayed multiple cracks, which broke the restoration and the tissues into multiple pieces (Failure type 2, 87.5%). In the majority of the cases, restoration remained bonded to enamel after fracture. In contrast, in Groups D the proportion between Failure type 1 and 2 was more balanced, respectively 40% and 60%. In almost all these fractures there was a large debonding of the restoration to dentine substrate (Table 4). Type 1 fractures were more current in thinner restorations (0.5 mm).

Fractographic analysis revealed a damage competition between cone/median cracks originating close to the loading contact area of the restorations and radial cracks beginning at their inner surface, with cone/median cracking prevailing in restorations bonded on enamel (E groups) (Fig. 4) and radial cracks being dominant for restorations bonded on dentine (D groups) (Figs. 5 and 6). A correlation between the thickness of the restorative material and the type of fracture was also detected, with radial cracking more present in thinner restorations.

The results of the FEA for the 0.5D, 0.5E, 2D and 2E specimens are presented in Table 5 and Fig. 7. In modelled samples with thinner restorations, maximum principal stresses (MPSs) were more concentrated at the top/bottom of the restoration and at the bonding interface when the restoration was bonded to dentine (0.5D), whereas higher tension was observed at the top of the restoration and into the enamel in the enamel substrate equivalent sample (0.5E). In modelled thicker specimen 2D, the MPS pattern was similar to the respective thinner specimen 0.5D, but with higher values, above all at the restoration top and into the cement. In modelled specimen 2E, the MPS pattern was similar to specimen 0.5E but more exacerbated into the enamel.

4. Discussion

In the present study, the fracture strength and behaviour after fracture of a novel CAD-CAM resin composite material tested at different thicknesses and bonded to different dental substrates was investigated. Within the limitations of this study, results showed a linear relation between restoration thickness and its load-bearing capacity regardless of the substrate, while the bonding substrate showed an impact limited to fracture resistance of thin restorations. Thus, in terms of resistance to a quasi-static load, the null hypothesis a) was rejected and the b) was partially rejected (except for 2 mm-thick restorations). When considering the fracture behaviour of restorations, null hypothesis a) and b) were rejected.

A Hertzian load-to-failure contact test with a spherical contact indenter over a flat-layer structure was used. This test allows simple and standardized experimentation [4,12,34]. On the contrary, testing with a small radii indenter (5 mm), such as the one used, can generate intense point loads, which are more likely to create surface damage rarely detected in clinics [35].

Specimens were built as bi- and tri-layer structures in which circular flat restorations at different thicknesses were bonded on cylinders of bovine dentine (Group D) or dentine and enamel (Group E) (Fig. 1). The diameter of the restorative discs and therefore of the whole assembly was set at 9 mm, similar to the average dimensions of a molar [36]. The restorative discs were milled from a novel industrially polymerized CAD-CAM

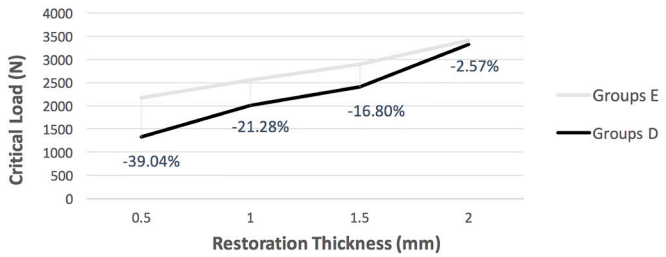

Fig. 3. Means of critical load values and percentage of difference between these values for specimens of Groups E and D with the same restoration thickness.

Table 4. Macroscopic types of restoration failure after the strength test (n=10). Type 1 failure: the crack broke the restoration without damaging the subjacent tissues and provoked partial/total restoration debonding; Type 2 failure: the fracture involved both restoration and the subjacent tissues.

	Groups E				Groups D			
Restoration Thickness	0.5 mm	1 mm	1.5mm	2 mm	0.5 mm	1 mm	1.5 mm	2 mm
Failure type 1	3	1	1	0	7	3	4	3
Failure type 2	7	9	9	10	3	7	6	7

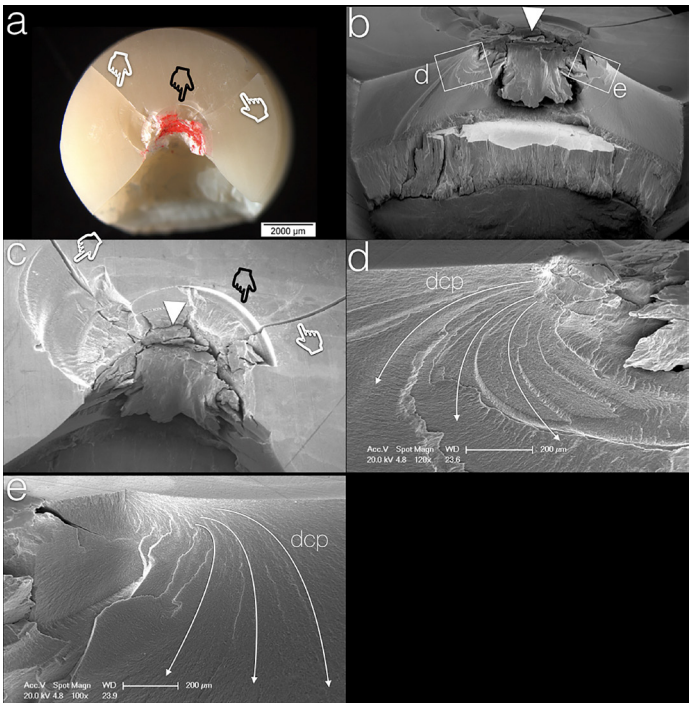

Fig. 4. Specimen from Group 1.5E. A typical fracture of a restoration bonded to enamel. Failure type 2 (a) A stereomicroscope image from the top of the fractured specimen. The red mark indicates the impact area. The white indexes indicate visible median cracks while the black one the cone cracking. The fracture passed through the entire specimen (Mode 2) but a large portion of the restoration is still in place. (b) SEM front view of the fractured surface. White tip designates the loading contact and the main origin of the fracture. (c) The impact area from the top. White and black indexes indicate median and cone cracks respectively. (d) and (e) White arrows indicate the direction of crack propagation (dcp). Both in the left and in the right front of the fracture, the crack starts at the surface of the restoration and at the loading contact area and propagates downwards to the restoration's boundaries.

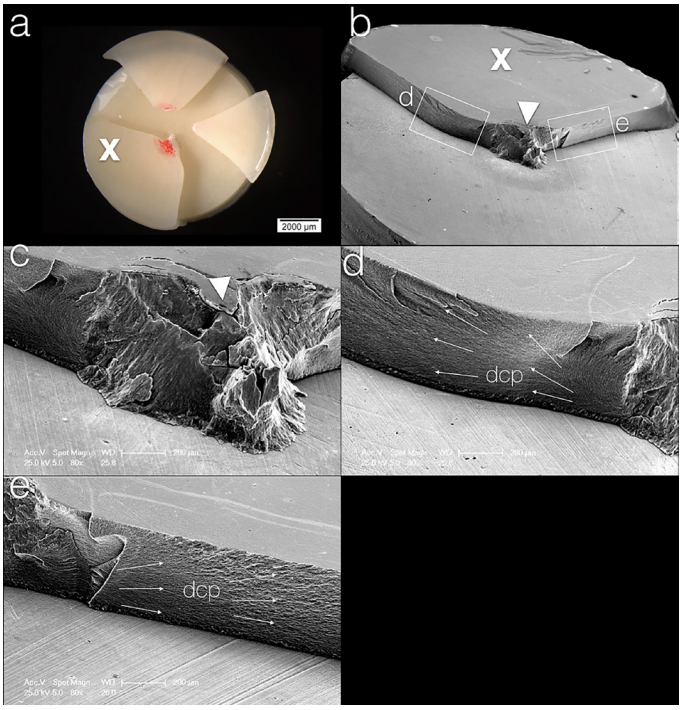

Fig. 5. Specimen from Group 0.5D. A typical fracture of an ultra-thin restoration bonded to dentin. Failure type 1. (a) Picture from the stereomicroscope of the fractured surface from the top. The restoration fractured in multiple pieces which debonded at the cement/dentin interface leaving practically the whole dentin surface intact. The red surface indicates the main loading contact. Letter X indicates the investigated segment. (b) A SEM view of the fracture. The white tip indicates the impact area. Both the left and the right part of the fracture surface are marked by radial cracking. (c) A SEM large view of the impact area. (d) and (e) White arrows indicate the direction of crack propagation (dcp). The radial cracks start at the bottom of the plastic deformation area (cement/dentin interface) underneath the loading contact and ran to the restoration top surface and boundaries.

Table 5. Table showing highest Maximum Principal Stress values (MPa) observed at main stress concentration zones.

	Restoration (top)	Restoration (bottom)	Cement	Enamel (top)	Dentin (top)
Model 0.5E	57 MPa	12 MPa	8 MPa	118 MPa	..
Model 0.5D	40 MPa	33 MPa	27 MPa	..	27 MPa
Model 2E	38 MPa	7 MPa	8 MPa	149 MPa	..
Model 2D	106 MPa	56 MPa	90 MPa	..	69 MPa

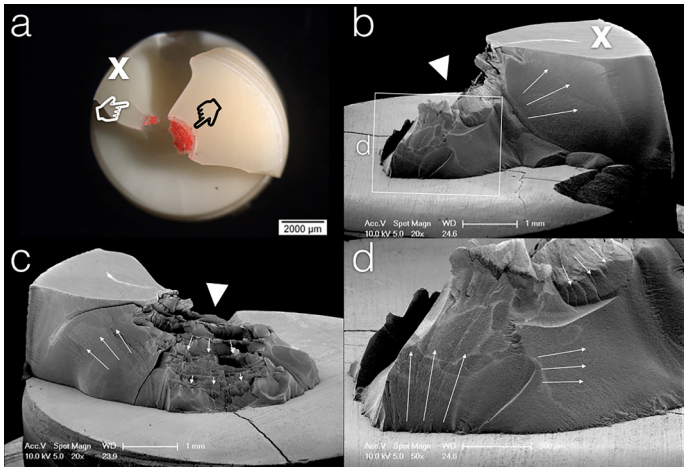

Fig. 6. Specimen from Group 2D. A typical fracture of a thicker restoration bonded to dentin. Failure type 2 (a) Spectrophotometric image from the top of the specimen. The fracture provoked the almost entire debonding of the restoration. The letter X indicates the analysed fragment. White and black indexes denote median and cone cracks respectively. (b) and (c) SEM images of the right and left sides of the fractured surface. White arrows indicate the direction of crack propagation. The competition between cone and median cracks (direction downwards) and radial cracks (direction upwards) is evident. (d) higher magnification of the area below the loading impact.

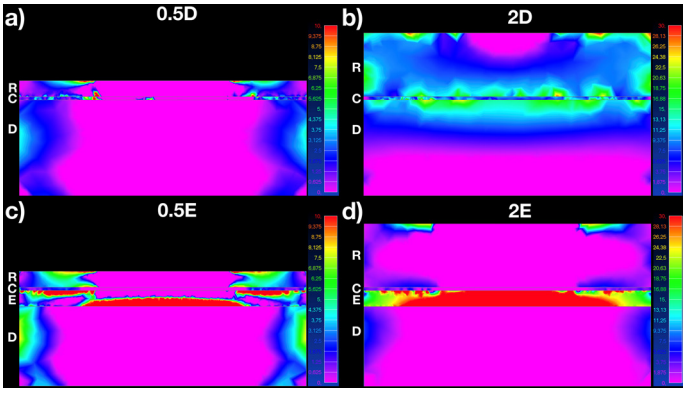

Fig. 7. Image showing lateral cuts with Maximum Principal Stress values (MPa) inside the models. The mean fracture load obtained in the fracture strength test was applied to the FEA models.
R: restoration; C: cement; E: enamel; D: dentin.

composite resin material (Brilliant Crios, Coltène/Whaledent AG). Being polymerized under controlled high-pressure/high-temperature conditions, the composite resin produced is highly homogeneous and, therefore, its mechanical properties are higher than the chair-side photopolymerized resin equivalents [37]. Bovine enamel and dentine have been widely validated as human substitutes in laboratory research for their adhesive and mechanical properties [38]. The use of these tissues in the form of a cylindrical base in the present flat-layer model offers a better standardization of specimens than testing on extracted human teeth. The thickness of the tissue base was 3 mm and maintained constant for all specimens to avoid any impact of the base dimensions over the resistance to fracture of the bonded restoration. The association of this flat-layer model with a simple Hertzian monotonic testing gave a high degree of standardization to the study. This statement is supported by the low coefficient of variation (CV) of fracture strength testing values in all groups (Table 3).

Results of the quasi-static fracture strength test displayed increased values of the critical load of the tested restorations with the increase of their thickness, when they were bonded to either enamel or to dentine (Table 3 and Fig. 3). Specimens with 0.5 mm-thick restorations bonded on enamel had a 36.26 % less resistance to fracture compared to specimens with 2 mm-thick restorations (0.5E vs 2E), whereas in specimens with dentine substrate this difference increased up to 60.11% (0.5D vs 2D).

This difference progressively decreased for 1.5 mm- and for 1 mm-thick restorations. This means that there was a clear linear positive relationship between fracture strength and restoration thickness for both the substrates, and this relationship was more evident for restorations bonded to dentine. These results are not in agreement with a previous study conducted in similar testing conditions by Chen et al. [4] where the authors found no differences in terms of load-bearing capacity between flat CAD-CAM resin nano-ceramic restorations (LAVA Ultimate, 3M, St. Paul, MN, USA) of 0.5 mm and 2 mm, bonded over resin dentine analogous cylinders. However, in that study, the modulation of the thickness of the resin cylinder base according to the variation in thickness of the bonded restoration to keep the final dimensions of the specimen unvaried, could have produced this non-linear correlation between restoration thickness and its critical load. With regard to the differences in strength values between bonding substrates for the same restoration thickness, specimens with restorations of 0.5, 1 and 1.5 mm bonded to dentine (namely 0.5D, 1D and 1.5D) presented a significant lower resistance to fracture of 39.04%, 21,28% and 16.80% less than 0.5E, 1E and 1.5E, respectively (Fig. 3). Nevertheless, this difference was not statistically significant within specimens with 2 mm-thick restorations – mean fracture strength value of 2D was just 2.57% less than that of 2E − which suggests that the influence of the substrate is evident in thin restorations and gradually decreases as the restoration thickens.

A fractographic analysis was carried out on all fragments to investigate the events that took place during the specimens' fractures. A combined stereo and scanning electron microscopy technique was used. While stereomicroscope revealed a better 3D vision of the fractured surface, SEM images efficiently provided the information on characteristic fractographic markers, such as hackle lines, arrest lines and wake hackle, which are indicators of the crack propagation direction [39,40].

Cone and median cracks were more frequent when restoration was bonded to enamel, no matter how thick the restoration was (Fig. 4). The main median crack originated at the loading contact area and progressed downwards through the restoration and then into tissues (Failure type 2), breaking the specimen into two halves (or in a portion) with sporadic restoration debonding. A zone of plastic permanent deformation was present beneath the main loading contact, where the median crack initiated. Tensile stress concentration below this zone leads to rapid microcrack coalescence generating the main crack [41]. In some specimens of Group 0.5E, the main crack originated at the inner surface of the restoration as an upgoing radial crack, as an exception. In all specimens of groups E, several secondary median and cone cracks were also visible over the restoration surface.

In contrast, radial crack was the prevailing damage mode in ultra-thin restorations bonded to dentine (Groups 0.5D). Very few secondary cone and median cracks were visible over the restoration surface. In fact, the bending under stress of the coating over the thick compliant substrate (dentine) initiated radial cracks, which spread upwards and outwards from the cement−dentine interface below the plastic deformation area, provoking restoration fracture. Some of these radial cracks propagated perpendicularly to the loading direction into the cement−dentine bonding interface, initiating the debonding of a large portion of the restoration. The spreading of these radial cracks upwards avoided the crack extension into the dentine layer (Failure type 1, 70%) (Fig. 5). The above-mentioned damage competition between cone/median and radial cracks, which differentiated the mode of fracture of ultra-thin restorations bonded to enamel (Group 0.5E) or dentine (Group 0.5D) substrates, respectively, could explain their high discrepancy in terms of fracture strength as in brittle materials lower critical loads are needed to trigger radial cracks [19].

The gradual increase in the thickness of the restorative coating attenuated progressively the difference in terms of fracture strength and fracture behaviour between specimens of groups E and D (Fig. 3). In fact, specimens of Group 2D broke into multiple pieces and the mode of fracture was mainly the Failure type 2. Radial cracks were dominant in these specimens but downcoming median cracks starting from the zone of impact (plastic deformation) were often detected on the fractured surfaces,

contrary to what was described before for thinner specimens of Group 0.5D and similar to broken specimens of groups E (Fig. 6). This similarity in fracture behaviour between thicker specimens of groups E and D could elucidate their similar fracture strength mean values. On the other hand, the rate of debonding of fractured fragments of Group 2D was still higher than for fragments of Group 2E.

Difference in E-modulus between enamel and dentine and changes in thickness of the restorations could explain the aforementioned dynamics of fracture. In fact, in the modelled specimen with ultra-thin restoration bonded to enamel 0.5E, FEA showed that MPSs are concentrated above all at the restoration's top surface and into the enamel, with practically no stresses into the cement layer, as stiff enamel absorbs stresses and avoids bending. This stress pattern enlightens the predominance in vitro in these specimens of downcoming median/cone cracks beginning at the occlusal contact area, which broke the restorations and the subjacent tissues without almost any debonding. On the other hand, in the modelled specimen of ultra-thin restoration bonded to dentine 0.5D, stress concentration under load is equally distributed within restoration top/bottom, the cement layer and dentine, due to the increased elasticity of the dentine substrate. This stress pattern clarifies the prevalence in vitro in these specimens of radial cracks coming from the restoration/dentine interface and the high rate of restoration debonding. In the thicker modelled specimen 2E, distribution of MPS is similar to the respective thinner specimen 0.5E, which could explain the similarity in terms of fracture behaviour in vitro between specimens of these two groups. In modelled specimen 2D, the rigidity of the specimen increases due to the increase in thickness of the restoration. The MPS pattern of 2D is similar to 0.5D but with an increase in tension above all at the top of the restoration and into the cement. This pattern could explain the simultaneous presence in fractured specimens of this Group of radial, cone and median cracks.

Clinically, results of this study suggest that enamel, as a bonding substrate, assures higher critical loads to fracture than dentine to bonded thin resin composite restorations. Conservation of enamel and, therefore, early diagnostic and therapy are crucial when treating eroded/worn posterior teeth with CAD-CAM resin composite overlays. At the same time, beyond a specific threshold of thickness – 2 mm in the present study − resin restorations become rigid enough to not be affected by the bonding substrate, similarly to fracture mechanics of veneered feldspathic ceramics. As a matter of fact, mean fracture strength value of 2-mm thick restorations bonded to dentin was just 2.57% less than 2-mm thick restorations bonded to enamel. All tested specimens met the minimal resistance requirements – more than 1000 N [42] – to counteract monotonic accidental biting forces. Although high load-to-fracture values obtained with this in vitro set-up, namely quasi-static/uniaxial extreme loading over one central occlusal contact, should not be used to predict clinical mechanical limits of different restorations, as in the clinical setting, restorations are known to fail more frequently in fatigue conditions under cyclic/multiaxial physiological loadings with multiple contact areas. Both high failure loads and the extreme surface contact damages obtained with the Hertzian indentation used in this study are rarely detected in clinics. Also, while the applied simplified bi- and tri-layer overlay model on the one hand guarantees high standard levels, on the other it is unable to mimic the complex geometry of a dental crown.

The bond strength of the adhesive interface between restorations and the tissue substrate − enamel or dentine − is known to have an influence over restorations' critical loads [43,44]. It is important to note that in this study this issue was not explored. A universal adhesive system was applied (One Coat 7 Universal, Coltène/Whaledent AG) to both enamel and dentine, with a previous orthophosphoric acid etching of enamel. The immediate bond strength of 'universal' self-etching adhesive systems to enamel and dentine has been previously shown as being similar [45]. Nevertheless, in this study the debonding of restorations after fracture was always more extensive in 'dentine' specimens than in 'enamel' ones, no matter the thickness of the restorations. As the crack chooses constantly the easier path during its run, it is reasonable to suppose that in this in vitro set-up the adhesive interface to dentine was weaker compared to the enamel interface. A preliminary immediate bond strength test on these specimens would have been necessary to validate this hypothesis and correlate bonding effectiveness to fracture strength values and fracture behaviour.

5. Conclusion

Within the limits of this in vitro study it was concluded that:

The tooth substrate has an impact on critical loads of thin CAD-CAM composite resin restorations. Within a thickness range of the composite resin restoration of 0.5 mm to 1.5 mm, enamel as a bonding substrate assures higher restoration fracture strength than dentine. This impact gradually diminishes as the restoration becomes thicker.

Both the bonding tooth substrate and the thickness of the restoration have an influence on the fracture behaviour of veneered composite resin restorations. The majority of the restorations bonded to enamel displayed multiple cracks, which broke the restoration and the subjacent tissues into multiple pieces. In most of the cases the restoration remained bonded to enamel after fracture. Contrariwise, in specimens with restoration bonded to dentine, the proportion between cracks that penetrated and cracks that did not penetrate tissues was more balanced. In almost all these fractures there was a large debonding of the restoration to dentine substrate.

With regard to the correlation between the thickness of the restorative material and the type of fracture, radial cracking and cracks that did not penetrated tissues (Failure type 1) were more frequent in 0.5-mm ultra-thin restorations.

Further in vitro studies and clinical trials are needed to confirm these results. In particular results obtained for the specific CAD-CAM composite resin tested in this study should not be safely generalised to all CAD-CAM composite resin materials present today on the market which may vary in properties and, in future, these outcomes should be also compared with CAD-CAM ceramic materials.

Conflicts of interest

The authors declare no conflicts of interest related to the materials used in the present study.

Acknowledgements

The authors wish to thank Coltène and Kuraray for their generous supply of the tested materials. This work was supported by the Swiss Dental Association (SSO), grant number 296-17.

References

[1] Rocca GT, Rizcalla N, Krejci I, Dietschi D. Evidence-based concepts and procedures for bonded inlays and onlays. Part II. Guidelines for cavity preparation and restoration fabrication. Int J Esthet Dent 2015;10:392–413.
[2] Vailati F, Belser UC. Full-mouth adhesive rehabilitation of a severely eroded dentition: the three-step technique. Part 1. Eur J Esthet Dent 2008;3:30–44.
[3] Lawn BR, Deng Y, Miranda P, Pajares A, Chai H, Kim DK. Overview: Damage in brittle layer structures from concentrated loads. J Mater Res 2002;17:3019–36. https://doi.org/10.1557/JMR.2002.0440.
[4] Chen C, Trindade FZ, de Jager N, Kleverlaan CJ, Feilzer AJ. The fracture resistance of a CAD/CAM Resin Nano Ceramic (RNC) and a CAD ceramic at different thicknesses. Dent Mater 2014;30:954–62. https://doi.org/10.1016/j.dental.2014.05.018.
[5] Johnson AC, Versluis A, Tantbirojn D, Ahuja S. Fracture strength of CAD/CAM composite and composite-ceramic occlusal veneers. J Prosthodont Res 2014;58:107–14. https://doi.org/10.1016/j.jpor.2014.01.001.
[6] Magne P, Knezevic A. Thickness of CAD–CAM composite resin overlays influences fatigue resistance of endodontically treated premolars. Dent Mater 2009;25:1264–8. https://doi.org/10.1016/j.dental.2009.05.007.
[7] Guess PC, Schultheis S, Wolkewitz M, Zhang Y, Strub JR. Influence of preparation design and ceramic thicknesses on fracture resistance and failure modes of premolar partial coverage restorations. J Prosthet Dent 2013;110:264–73. https://doi.org/10.1016/S0022-3913(13)60374-1.
[8] Skouridou N, Pollington S, Rosentritt M, Tsitrou E. Fracture strength of minimally prepared all-ceramic CEREC crowns after simulating 5 years of service. Dent Mater 2013;29:e70–7. https://doi.org/10.1016/j.dental.2013.03.019.

[9] Sasse M, Krummel A, Klosa K, Kern M. Influence of restoration thickness and dental bonding surface on the fracture resistance of full-coverage occlusal veneers made from lithium disilicate ceramic. Dent Mater 2015;31:907–15. https://doi.org/10.1016/j.dental.2015.04.017.
[10] Magne P, Schlichting LH, Maia HP, Baratieri LN. In vitro fatigue resistance of CAD/CAM composite resin and ceramic posterior occlusal veneers. J Prosthet Dent 2010;104:149–57. https://doi.org/10.1016/S0022-3913(10)60111-4.
[11] Abu-Izze FO, Ramos GF, Borges ALS, Anami LC, Bottino MA. Fatigue behavior of ultrafine tabletop ceramic restorations. Dent Mater 2018;34:1401–9. https://doi.org/10.1016/j.dental.2018.06.017.
[12] Monteiro JB, Riquieri H, Prochnow C, Guilardi LF, Pereira GKR, Borges ALS, et al. Fatigue failure load of two resin-bonded zirconia-reinforced lithium silicate glass-ceramics: Effect of ceramic thickness. Dent Mater 2018;34:891–900. https://doi.org/10.1016/j.dental.2018.03.004.
[13] Schlichting LH, Maia HP, Baratieri LN, Magne P. Novel-design ultra-thin CAD/CAM composite resin and ceramic occlusal veneers for the treatment of severe dental erosion. J Prosthet Dent 2011;105:217–26. https://doi.org/10.1016/S0022-3913(11)60035-8.
[14] Kelly JR. Clinically relevant approach to failure testing of all-ceramic restorations. J Prosthet Dent 1999;81:652–61. https://doi.org/10.1016/S0022-3913(99)70103-4.
[15] Lawn BR, Lee KS, Chai H, Pajares A, Kim DK, Wuttiphan S, et al. Damage-Resistant Brittle Coatings. Adv Eng Mater 2000;2:745–8. https://doi.org/10.1002/1527-2648(200011)2:11<745::AID-ADEM745>3.0.CO;2-E.
[16] Lee KS, Wuttiphan S, Hu X-Z, Lee SK, Lawn BR. Contact-Induced Transverse Fractures in Brittle Layers on Soft Substrates: A Study on Silicon Nitride Bilayers. J Am Ceram Soc 2005;81:571–80. https://doi.org/10.1111/j.1151-2916.1998.tb02376.x.
[17] Scherrer SS, de Rijk WG, Belser UC, Meyer JM. Effect of cement film thickness on the fracture resistance of a machinable glass-ceramic. Dent Mater 1994;10:172–7. https://doi.org/10.1016/0109-5641(94)90028-0.
[18] Tsai YL, Petsche PE, Anusavice KJ, Yang MC. Influence of glass-ceramic thickness on Hertzian and bulk fracture mechanisms. Int J Prosthodont 1998;11:27–32.
[19] Lawn BR, Pajares A, Zhang Y, Deng Y, Polack MA, Lloyd IK, et al. Materials design in the performance of all-ceramic crowns. Biomaterials 2004;25:2885–92. https://doi.org/10.1016/j.biomaterials.2003.09.050.
[20] Øilo M, Quinn GD. Fracture origins in twenty-two dental alumina crowns. J Mech Behav Biomed Mater 2016;53:93–103. https://doi.org/10.1016/j.jmbbm.2015.08.006.
[21] Hermann I, Bhowmick S, Zhang Y, Lawn BR. Competing fracture modes in brittle materials subject to concentrated cyclic loading in liquid environments: Trilayer structures. J Mater Res 2006;21:512–21. https://doi.org/10.1557/jmr.2006.0056.
[22] Rocca GT, Krejci I. Bonded indirect restorations for posterior teeth: from cavity preparation to provisionalization. Quintessence Int (Berl) 2007;38:371–9.
[23] Belli R, Petschelt A, Lohbauer U. Are linear elastic material properties relevant predictors of the cyclic fatigue resistance of dental resin composites. Dent Mater 2014;30:381–91. https://doi.org/10.1016/j.dental.2014.01.009.
[24] Biswas N, Dey A, Kundu S, Chakraborty H, Mukhopadhyay AK. Mechanical Properties of Enamel Nanocomposite. ISRN Biomater 2013;2013:1–15. https://doi.org/10.5402/2013/253761.
[25] Xu HHK, Smith DT, Jahanmir S, Romberg E, Kelly JR, Thompson VP, et al. Indentation Damage and Mechanical Properties of Human Enamel and Dentin. J Dent Res 1998;77:472–80. https://doi.org/10.1177/00220345980770030601.
[26] AL-Makramani BMA, Razak AAA, Abu-Hassan MI. Evaluation of Load at Fracture of Procera AllCeram Copings Using Different Luting Cements. J Prosthodont 2008;17:120–4. https://doi.org/10.1111/j.1532-849X.2007.00270.x.
[27] Kurtoglu C, Uysal H, Mamedov A. Influence of Layer Thickness on Stress Distribution in Ceramic-Cement-Dentin Multilayer Systems. Dent Mater J 2008;27:626–32. https://doi.org/10.4012/dmj.27.626.
[28] Fleming GJP, Cao X, Romanyk DL, Addison O. Favorable residual stress induction by resin-cementation on dental porcelain. Dent Mater 2017;33:1258–65. https://doi.org/10.1016/j.dental.2017.07.018.
[29] Addison O, Marquis PM, Fleming GJ. Quantifying the strength of a resin-coated dental ceramic. J Dent Res 2008;87:542–7. https://doi.org/10.1177/154405910808700610.
[30] Qin QH, Zhang X. Crack deflection at an interface between dissimilar piezoelectric materials. Int J Fract 2000;102:355–70. https://doi.org/10.1023/A:1007601312977.
[31] Parmigiani J, Thouless M. The roles of toughness and cohesive strength on crack deflection at interfaces. J Mech Phys Solids 2006;54:266–87. https://doi.org/10.1016/j.jmps.2005.09.002.
[32] Magne P, Knezevic A. Simulated fatigue resistance of composite resin versus porcelain CAD/CAM overlay restorations on endodontically treated molars. Quintessence Int 2009;40:125–33.
[33] Zhu JJ, Tang ATH, Matinlinna JP, Hägg U. Acid etching of human enamel in clinical applications: A systematic review. J Prosthet Dent 2014;112:122–35. https://doi.org/10.1016/j.prosdent.2013.08.024.
[34] Lawn BR, Deng Y, Thompson VP. Use of contact testing in the characterization and design of all-ceramic crownlike layer structures: A review. J Prosthet Dent 2001;86:495–510. https://doi.org/10.1067/mpr.2001.119581.
[35] Kelly JR, Rungruanganunt P, Hunter B, Vailati F. Development of a clinically validated bulk failure test for ceramic crowns. J Prosthet Dent 2010;104:228–38. https://doi.org/10.1016/S0022-3913(10)60129-1.
[36] Ferrario VF, Sforza C, Tartaglia GM, Colombo A, Serrao G. Size and shape of the human first permanent molar: A Fourier analysis of the occlusal and equatorial outlines. Am J Phys Anthropol 1999;108:281–94. https://doi.org/10.1002/(SICI)1096-8644(199903)108:3<281::AID-AJPA4>3.0.CO;2-#.
[37] Ruse ND, Sadoun MJ. Resin-composite Blocks for Dental CAD/CAM Applications. J Dent Res 2014;93:1232–4. https://doi.org/10.1177/0022034514553976.
[38] Yilmaz ED, Koldehoff J, Schneider GA. On the systematic documentation of the structural characteristics of bovine enamel: A critic to the protein sheath concept. Dent Mater 2018;34:1518–30. https://doi.org/10.1016/j.dental.2018.06.006.
[39] Scherrer SS, Quinn JB, Quinn GD, Wiskott HWA. Fractographic ceramic failure analysis using the replica technique. Dent Mater 2007;23:1397–404. https://doi.org/10.1016/j.dental.2006.12.002.
[40] Rocca GT, Sedlakova P, Saratti CM, Sedlacek R, Gregor L, Rizcalla N, et al. Fatigue behavior of resin-modified monolithic CAD–CAM RNC crowns and endocrowns. Dent Mater 2016;32:e338–50. https://doi.org/10.1016/j.dental.2016.09.024.
[41] Lee JJ-. W, Kwon J-Y, Chai H, Lucas PW, Thompson VP, Lawn BR. Fracture Modes in Human Teeth. J Dent Res 2009;88:224–8. https://doi.org/10.1177/0022034508330055.
[42] Waltimo A, Könönen M. A novel bite force recorder and maximal isometric bite force values for healthy young adults. Eur J Oral Sci 1993;101:171–5. https://doi.org/10.1111/j.1600-0722.1993.tb01658.x.
[43] Furukawa K, Inai N, Tagami J. The effects of luting resin bond to dentin on the strength of dentin supported by indirect resin composite. Dent Mater 2002;18:136–42. https://doi.org/10.1016/S0109-5641(01)00032-X.
[44] Wang Y, Katsube N, Seghi RR, Rokhlin SI. Statistical failure analysis of adhesive resin cement bonded dental ceramics. Eng Fract Mech 2007;74:1838–56. https://doi.org/10.1016/j.engfracmech.2006.11.006.
[45] Makishi P, André C, Ayres A, Martins A, Giannini M. Effect of Storage Time on Bond Strength and Nanoleakage Expression of Universal Adhesives Bonded to Dentin and Etched Enamel. Oper Dent 2016;41:305–17. https://doi.org/10.2341/15-163-L.